Cell Biochemistry and Biophysics
https://doi.org/10.1007/s12013-024-01480-w

ORIGINAL PAPER

Role and Molecular Mechanism of miR-586 in the Differentiation of Dental Pulp Stem Cells into Odontoblast-like Cells

Gang Pan[1] · Qianwen Zhou[1] · Chenhua Pan[2] · Yingxue Zhang[1]

Accepted: 2 August 2024

Abstract

Dental pulp stem cells (DPSCs) are a class of cells with the potential of self-replication and multi-directional differentiation, which are widely considered to have great application value. It was to investigate miR-586 in DPSCs differentiated into odontoblast-like cells. In this article, human dental pulp stem cells (hDPSCs) were used as samples, and hDPSCs were co-cultured with endothelial progenitor cells (EPCs). Furthermore, a lentiviral expression vector for the miR-586 inhibitor was established. The effect of miR-586 inhibitor expression vector on the activity of hDPSCs was detected by Cell Counting Kit-8 (CCK-8). The differentiation of hDPSCs was tested by mineralized nodule staining. The expression of miR-586 and a gene related to dental cell differentiation in the pulp was subjected to detection by real-time quantitative PCR (qRT-PCR). As against the normal hDPSCs and the empty vector, the miR-586 lentivirus expression inhibition vector could visibly raise the expression of dentin sialophosphoprotein (DSPP) in hDPSCs; and the cell proliferation activity was visibly enhanced; In addition, the mRNA expressions of dentin-matrix acidic phosphoprotein 1 (DMP-1) and alkaline phosphatase (ALP) were visibly raised in the miR-586 lentivirus expression inhibition vector (all $P < 0.05$). Additionally, ALP activity was significantly enhanced ($P < 0.05$). The number of mineralized nodules was significantly increased ($P < 0.05$). MiR-586 plays a key regulatory function in DPSCs differentiated into odontoblast-like cells and is associated with specific molecular mechanisms.

Keywords miR-586 · hDPSCs · Odontoblasts · Cell differentiation · Lentiviral expression vector

Introduction

A common class of diseases in the oral cavity is endodontic disease, which usually leads to the damage of dental pulp tissue (DPT) due to irreversible inflammatory reaction, liquefaction, or necrosis. Ultimately, it is necessary to remove the affected DPT and perform root canal therapy to restore the function of the tooth and relieve the pain [1]. With the rapid development of tissue engineering technology, regenerative medicine has entered the field of stomatology. Scholars are paying more attention to the research of regenerative medicine in oral endodontic diseases, especially the pulp growing. In the field of dentistry, the treatment of endodontic diseases is no longer only about removing the damaged pulp and repairing with exogenous materials, but also promoting the DPT regenerating in the tooth body by eliminating the source of infection to replace the damaged pulp, or even to realize the whole tooth regenerating [2].

Cell therapy is the core of regenerative medicine. In dental pulp regeneration research, seed cells, scaffold materials, and cytokines are all essential elements in tissue engineering. When exploring tissue regeneration, most seed cells are stem cells of choice [3–5]. DPSCs exist in DPT. When the DPT is damaged, the undifferentiated mesenchymal cells can differentiate into a variety of different cell types according to the need, and may even directly differentiate into dentin cells, and eventually form a composite structure to repair the damaged DPT or dentin. hDPSCs can differentiate into osteoblasts, chondrocytes, etc [6]. HDPSCs are also related to immune regulation [7]. A study, has found that hDPSCs can change the proportion of T lymphocytes [8]. In another study, has shown that

✉ Yingxue Zhang
Zhangyingxue@mjc-edu.cn

[1] Department of Stomatology, PuRen Hospital, Wuhan University of Science and Technology, Wuhan 430081 Hubei Province, China

[2] Biological Cell Therapy Research Center, PuRen Hospital, Wuhan University of Science and Technology, Wuhan 430081 Hubei Province, China

Published online: 16 August 2024

co-culturing endothelial progenitor cells (EPS) with human dental pulp stem cells (hDPSCs) can enhance in vitro angiogenesis, which is of significant importance for the repair and regeneration of dental pulp tissue [9]. In the hDPSCs/EPS co-culture system, tumor necrosis factor-α(TNF-α) can significantly increase the total length of tubular branches and the number of branches formed, thereby establishing a robust cellular model. Odontoblasts are able to secrete dentin matrix, which is the main hard tissue of teeth formed by differentiated odontoblasts [10]. The dentin-specific protein Dentin sialophosphoprotein (DSPP) acts in the mineralization of dentin and the differentiation of DPSCs into odontoblasts. DSPP can promote the mineralization process and repair the damaged DPT. Proteolytic enzymes catalyze the formation of dentin glycoprotein (DGP)/dentin sialoprotein (DSP) and phosphoprotein (DPP). DPP contains an Arg-Gly-Asp (RGD) motif and an abundant Ser-Asp/Asp-Ser repeat region. The DPP-RGD motif binds to integrin αVβ3 and activates intracellular signaling, thereby inducing cell differentiation [11].

MicroRNA is a kind of small non-coding RNA, which plays a regulatory function in key biological processes such as cell growth, differentiation, and apoptosis. microRNA can bind to the 3'UTR of the mRNA of its target gene and suppress the transcription and translation of the target gene. Studies have found that the upregulation of miR-20a can enhance the viability and migration ability of DPSCs, as well as promote the osteogenic/odontoblast differentiation potential of cells [12]. In the study of Wang et al. (2020) miR-125a-3p acts in the odontoblast differentiation of hDPSC through targeting Fyn [13]. This indicates that microRNAs act in the study of dental pulp regrowing. In recent years, miR-586 has gradually become the focus of research because it has shown an important regulatory function in many biological processes [14–16]. This article was to discuss the key role of miR-586 in DPSCs differentiated into odontoblast-like cells and how it accomplishes this function through the molecular mechanisms. It is hoped that it can bring more enlightenment and methods to oral regenerative medicine and provide better remedy methods for sick persons.

Materials and Methods

Research Materials

hDPSCs were purchased from Hefei Wanwu Biology Technology Co., LTD. (ATCC) with item number tings 95,188 and 5×10^5/T25 culture flask, with short tandem repeat (STR) profile. The cells were co-cultured with human endothelial progenitor cells (EPCs) in 5×10^5/T25 flasks (PC-022h), supplied by Wuhan SAIOS Biotechnology Co., LTD.

Primary cells of hDPSCs and EPCs were mailed in T25 culture flasks at 25 °C, and those were received and sterilized. Subsequently, fresh Dulbecco's modified eagle medium (DMEM) containing double antibody (penicillin 100 IU, streptomycin 10 μg/mL), with 10% fetal bovine serum (FBS), was applied to the hDPSCs T25 culture flask in an ultra-clean bench. The complete medium for EPCs was Microvascular Endothelial Cell Growth medium-2 (EGM-2-MV) having 10% FBS. The flasks were then placed in a cell incubator at 37 °C in 5% CO_2 to allow the suspended cells to adhere to the walls. 12 h later, the cells were collected into a centrifuge tube for centrifugation (1600r/10 min) to remove cell debris, and then subcultured at 1:3 after counting. All cells used in this study were passage 3 (P3) cells after culture.

Preparation and Packaging of Lentiviral Vector and Detection of Venom Titer

microRNA 586expression inhibition vector was constructed using GV232 vector. The construction and packaging of lentiviral vector and the preparation of venom were carried out by Beijing Sino Biological Co., LTD. miRNA sequence: UAUGCAUUGUAUUUUUAGGUCC, stem ring structure sequence: AUGGGGUAAAACCAUUAUGCAUUGUAUUUUUAGGUCCCAAUACAUGUGGGCCCUAAAAAU-ACAAUGCAUAAUGGUUUUUCACUCUUUAUCUUC-UUAU.The sequence of elements in the GV232 vector is H1-MCS-CMV-puromycin. Genomic DNA extracted from hDPSCs cells was used as a template, and microRNA 586 primers were amplified using PCR. The amplified product was then digested with the restriction enzymes AgeI and EcoRI, and the target gene fragment was recovered. To construct the microRNA 586 inhibitory expression lentiviral vector, a reverse complementary sequence was designed as described above. The synthesized primer powder was dissolved in annealing buffer, incubated in a 90 °C water bath for 15 min, and then allowed to cool naturally to room temperature. The sequence of elements in the vector is hU6-MCS-CMV-puromycin. The GV232 vector was then digested with the restriction enzymes AgeI and EcoRI at 37 °C for 2 h, and the linearized expression vector was recovered by gel extraction. The recovered target gene fragment and double-stranded DNA oligonucleotides were then ligated into the linearized expression vector under the following reaction conditions: a molar ratio of linearized vector DNA to enzyme-digested purified PCR product/double-stranded DNA oligonucleotides of 2:1.5, at 16 °C for 6 h. The ligation products were directly transformed into competent cells and plated on LB agar plates containing Amp, which were incubated overnight. Positive single colonies were picked and identified by colony PCR, followed by sequencing and alignment analysis of PCR-positive clones. Correctly aligned clones were considered successfully constructed plasmids.

The constructed GV232-microRNA 586 vector was transiently transfected into 293 T cells using Lipofectamine 2000 (Thermo Fisher Scientific Inc., USA). After 8 h of culture, the medium was discarded, and the infection mixture was washed with PBS, then fresh serum-containing medium was added and cultured for another 48 h. The supernatant was collected as the lentivirus.

Then, the titer of lentivirus was detected by dilution counting method, 293 T cells in good growth condition were seeded into 96-well plates at a density of 5×10^3 cells per well in a volume of 100 μL. Before infection, the viral samples to be tested were subjected to ten-fold serial dilutions. The procedure was as follows: eight sterile EP tubes were prepared, each containing 90 μL of cell culture medium. Ten microliters of the viral sample to be tested was added to the first tube and mixed thoroughly. Then, 10 μL from the first tube was transferred to the second tube and mixed thoroughly. This process was repeated until the last tube was diluted. The desired wells in the 96-well plate were selected, and the existing culture medium was aspirated. Ninety microliters of the diluted viral solution were added to each well, and the wells were properly labeled. The plate was then placed in an incubator. After 48 h of incubation at 37 °C with 5% CO_2, 100 μL of fresh culture medium was added. After an additional 24 h, 150 μL of fresh culture medium was added. At 96 h post-infection, the fluorescence expression was observed, and the number of fluorescent cells was counted. If the virus carried only puromycin resistance, puromycin at a concentration of 5 μg/mL was added 48 h post-infection. The cells were cultured for another 2 days, and cell growth was observed to calculate the number of resistant cells. The copy number of integrated lentivirus vector in DNA samples was measured and calibrated by the number of genomes to obtain the copy number of integrated virus per genome. Integration units per mL (IU/mL) were computed.

$$\mathrm{IU/mL} = (\mathrm{C} \times \mathrm{N} \times \mathrm{D} \times 1000)/\mathrm{V} \quad (1)$$

Note: C is the average number of virus copies integrated per genome; N is the number of cells at infection (about 1× 100,000); D is the dilution of viral vector; V is the volume number of diluted virus added.

According to calculations, the titer of lentivirus in this study was 8.61×10^6.

MiR-586 Expression Inhibited by Lentiviral Transfection of hDPSCs

hDPSCs were cultured in 6-well plates and grouped: miR-586inhibition, miR-586 mimic, Vector, and hDPSCs. Each group had 5 wells. The transfection efficiency was 76%.

miR-586 inhibition: hDPSCs in a plate with 6 wells for 24 h, the medium was removed, and then the mixture of virus solution and medium (the final concentration of virus solution was 5 μg/mL) was added for culture. Through 24 h, puromycin at a final concentration of 2 μg/mL was used for screening, and the cells were collected after 24 h.

miR-586 mimic: as mentioned above.

Vector: The medium was taken and the mixture of blank vector and medium was applied for culture.

hDPSCs: The medium was taken and the fresh medium was adopted.

Staining After Osteogenic Induction

Mineralized nodule staining for hDPSCs cell differentiation was as follows. On day 14 of mineralization induction in the five groups of cells, the culture medium was removed, and the cells were washed three times with PBS. Subsequently, fixation was carried out using 4% paraformaldehyde for 15 min, followed by another three washes with PBS. Then, each well was stained with 1 mL of 2% alizarin red at room temperature for 30 min. After removing the staining solution, the wells were washed three times with PBS and air-dried for microscopic examination.

ALP activity detection was as follows. Alkaline phosphatase staining reagents (Yekani Biotechnology Co., Ltd., Shanghai, China) were used for staining of cells in each group, strictly following the instructions provided with the staining kit. Positive results were indicated by the presence of blue precipitates in the cytoplasm.

RT-PCR

The relative expression (RE) of miR-586 and related protein mRNA expression were detected by RT-PCR in the three groups of cells collected.

Trizol method (Product number: R1200; Supplier: Solarbio) was used to extract total RNA, and the operation was carried out strictly according to the instructions of the kit. Cells cultured to 80% confluence in each group were collected using EP tubes. One milliliter of Trizol reagent was added to each tube to lyse the cells thoroughly. The lysate was then transferred to a 1.5 mL centrifuge tube and allowed to stand at room temperature for 5 min to ensure complete mixing and lysis. An equal volume of chloroform was added to the centrifuge tube, the cap was secured, and the mixture was shaken vigorously for 15 s to ensure thorough mixing. The centrifuge tube was then left at room temperature for 2–3 min, followed by centrifugation at 12,000 g for 15 min at 2–8 °C. The aqueous phase was transferred to a new 1.5 mL centrifuge tube, and an equal volume of isopropanol was added. The mixture was allowed to stand at room temperature for 10 min to facilitate RNA precipitation. The mixture was centrifuged at 12,000 g for 10 min at 2–8 °C, and the supernatant was discarded. The

RNA pellet was washed with 1 mL of 75% ethanol, vortexed, and centrifuged at 7500 g for 5 min at 2-8 °C. The supernatant was discarded, and the RNA pellet was air-dried at room temperature. The RNA pellet was then dissolved in RNase-free water to obtain the extracted RNA samples.

The RNA was then reverse transcribed into cDNA and adopted for experiments using a PCR quantification kit. The reference gene U6, F: 5'-CTCGCTTCGGCAGCACA-3', R: 5'-AACGCTTCACGAATTTGCGT-3'; miR-586 primers: F: 5'-ACACTCCAGCTGGGTATGCATTGTATT TTTAGGT-3', R: 5'-CTCAACTGGTGTCGTGGA-3'; PCR reaction system: miR-586 forward and reverse primers each 0.4 μL, Taq enzyme 10 μL, dNTP 2 μL, ddH_2O 7.2 μL. PCR reaction settings: denaturation at 95 °C for 30 s, annealing at 60 °C for 30 s, extension at 72 °C for 5 min, 30 cycles. The RE wascalculated using the $2^{-\Delta\Delta Ct}$ method.

WB to Detect Protein Expression

WB detection was performed using a kit from Wuhan Proteintech Group, China. miR-586 inhibition, miR-586 mimic, Vector, and hDPSCs were collected in Eppendorf (EP) tubes, then placed in an ice box, mixed with tissue lysate (RIPA), centrifugation was carried out (12000r/10 min), and the supernatant was collected. Bicinchoninic acid assay (BCA) was adopted to detect the protein concentration. Preparation of SDS-PAGE gels, the protein samples were electrophoresed, subjected to transfer to membranes, and blocked. The primary antibody was applied, incubation at 4 °C overnight, the secondary antibody was applied, incubation at 25 °C for 2 h, and the membranes were washed, followed by development. The absorbance (OD) of the bands was detected by Quantity One gel analysis software, and the protein expression was calculated as the ratio of the OD of the target protein band to GAPDH.

Dual-luciferase Assay

The bioinformatics website ENCOR I: RNA Interaction Encyclopedia was utilized to predict and analyze potential targets of miR-586. By comparing the 3'UTR sequence of DSPP with the binding site of miR-586, regions of sequence similarity were identified. Pairing results suggested that DSPP might be a potential target of miR-586. Subsequently, the 3'UTR sequence of DSPP with predicted target sites was inserted into the Pgl3 promoter vector for transfection into hDPSCs cells.

hDPSCs were seeded into 24-well plates. Fluorescent enzyme reporter vectors (0.12 μg) and 40 mmol/L miR-856 mimics were added for co-transfection into the cultured hDPSCs cells in the 24-well plate. A dual-luciferase reporter gene assay kit was employed for luciferase reporter gene detection. Forty-eight hours post-transfection, luciferase activity was measured in triplicate.

HDPSCs/EPCs Induced by Co-culture

Principle: DPSCs and EPCs may naturally interact in vivo, particularly during tissue repair and regeneration processes. Co-culturing allows these two cell types to directly interact in an in vitro environment, thereby simulating their interactions such as cell communication, signal transduction, and paracrine effects. EPCs are critical cells involved in angiogenesis, capable of migrating to injury sites and participating in new blood vessel formation. hDPSCs also play a crucial role in tissue repair, as they can differentiate into various cell types including osteoblasts and chondrocytes. Co-culturing these two cell types may enhance synergistic effects in promoting angiogenesis and tissue regeneration processes.

hDPSCs and EPCs were co-cultured in DMEM medium having 10% FBS and EGM-2-MV medium having 10% FBS at a ratio of 1:1, and then those in good condition were transferred to the plate with 6 wells at a number of 2×10^4/well for further culture. When the number was fully spread to 70%, the medium containing mineral-inducing components was adopted, and the culture was continued.

Cell grouping: hDPSCs, miR-586 inhibition, miR-586 mimic, hDPSCs/EPCs, Vector hDPSCs/EPCs, miR-586 inhibition/EPCs, miR-586 mimic/EPCs.

The induction of mineralization was stopped on the 4th, 7th, and 14th day of culture, and the cells without mineralization at the same time were adopted as the Ctrl. After the completion of mineralization induction, the original medium was removed, and the cells were rinsed with PBS for 2–3 times. 1 mL Trizol cell lysate was applied to each well, respectively, and the cells were collected into EP tubes and stored at −80 °C for later use.

Cell Activity

CCK-8 was adopted for detection of the activity of miR-586 inhibition, Vector, and hDPSCs at 0, 1, 3, 5, and 7 days. The normal hDPSCs were digested with miR-586 inhibition group and Vector group, respectively, and then 10 μL was collected for counting. About 4000 cells were seeded in each well of a 6-well plate, and each sample was repeated for 5 wells. 24 h later, CCK-8 was applied, and the cells were incubated at 25 °C for 30 min before enzyme-labeled detection (OD450). The assay was then repeated every 30 min for 5 times.

The RE of DSPP, DMP-1, and ALP mRNA Determined by RT-PCR

The RE of DSPP, DMP-1, and ALP mRNA in each group was determined on the 4th, 7th, and 14th day of mineralization induction. The detection procedure was the same as described in Subsection 2.6. DSPP primers F: 5'-TCACAAGGGAGAAGGGAATG-3', R: 5'-TGCCATTTGCTGTGATGTTT-3'; DMP-1 primers F: 5'-AGTGCCCAAGATACCACCAG-3', R: 5'-CATTCCCTCATCGTCCAACT-3'; ALP primers F: 5'-CCAAAGGCTTCTTCTTGCTG-3', R: 5'-CCACCAAATGTGAAGACGTG-3'.

DSPP Protein Expression Determined by WB

The protein expression of DSPP in each group was determined on the 4th, 7th, and 14th day of mineralization induction, and the total protein was extracted for SDS-PAGE gel electrophoresis. The assay procedure was the same as described in Subsection "RT-PCR".

Satirical Analysis

SPSS24.0 software (IBM Corp., Armonk, NY)was adopted for data processing, and the experimental results were presented as mean ± sd ($\overline{x} \pm s$). *t* test and ANOVA were adopted for contrast. $P < 0.05$ meant there was a visible distinction.

Results

High-definition Images of hDPSCs Cells

Figure 1 depicted high-definition microscopic images of hDPSCs cells, in which the cells were observed to exhibit a spindle-shaped morphology, with plump cell bodies and nuclei that were round or oval. Prominent polar processes were noted, and the cells tended to align uniformly.

MiR-586 Lentivirus Inhibition Vector on the RE of miR-586 in hDPSCs

The average RE of miR-586 in normal hDPSCs was $0.96/2^{-\Delta\Delta Ct}$. After the empty lentiviral vector was transfected into hDPSCs, the RE of miR-586 in vector was not visibly different from that in normal hDPSCs ($P > 0.05$). After the lentiviral vector carrying miR-586 gene was transfected into hDPSCs, the RE of miR-586 was visibly reduced as against normal hDPSCs ($P < 0.05$), and the relative expression level of miR-586 in the miR-586 mimic group of cells was significantly increased compared to normal hDPSCs cells ($P < 0.05$) (Fig. 2).

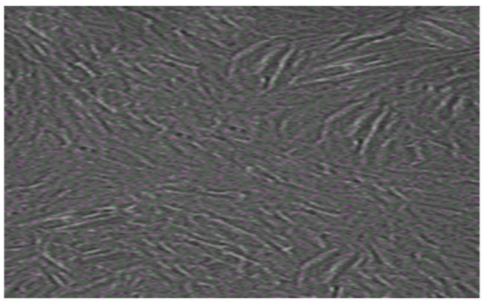

Fig. 1 High-definition image of hDPSCs cells (100×)

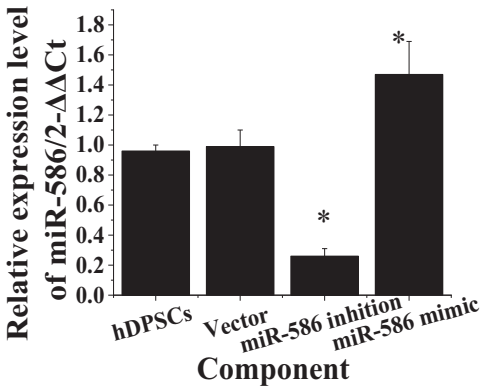

Fig. 2 Contrast of RE of miR-586. Note: As against hDPSCs, $*P < 0.05$

MiR-586 Lentivirus Inhibition Vector on the Expression of DSPP in hDPSCs

DSPP can promote the process of biomineralization and repair the damaged DPT, so the expression of DSPP was detected. The expression of DSPP in hDPSCs was similar to that in the Vector. The expression level of DSPP in the miR-586 inhibition group of cells was significantly increased compared to both the hDPSCs group and the Vector group ($P < 0.05$), indicating statistical significance. Conversely, the expression level of DSPP in the miR-586 mimic group of cells was significantly decreased compared to both the hDPSCs group and the Vector group ($P < 0.05$), also demonstrating statistical significance (Fig. 3).

Validation of miR-586mimic Targeting DSPP

The study identified binding sites between miR-586 and DSPP. Dual-luciferase reporter assay results (Fig. 4) revealed that co-transfection of miR-586 mimic with DSPP-WT significantly reduced luciferase activity in cells

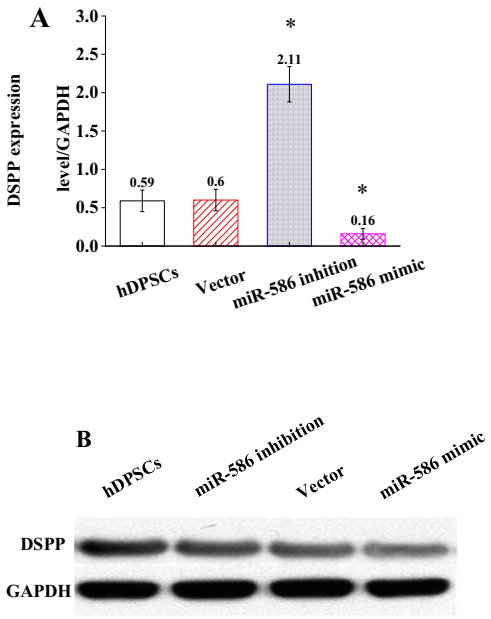

Fig. 3 Contrast of DSPP expression. (**A** represents the expression level of DSPP, while **B** represents the WB image of DSPP.). Note: As against hDPSCs, $*P < 0.05$

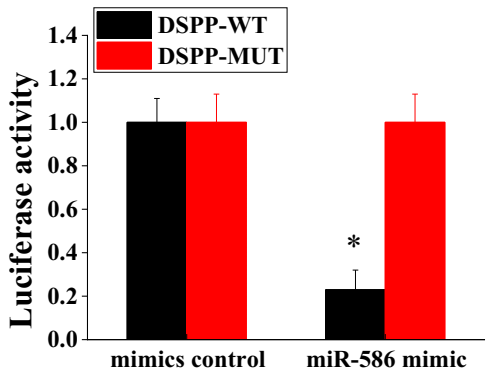

Fig. 4 Validation results of miR-586 mimic targeting DSPP. Note: compared to co-transfection with the mimic control, $*P < 0.05$

compared to the control group ($P < 0.05$), indicating a significant difference.

Suppressing miR-586 Expression on the Proliferation Activity of hDPSCs

Before CCK-8 experiment, there was similar in the OD in the three groups; From day 1 to day 7 following transfection, the proliferation activity suggested a gradual upward trend. On the first day, there was similar among the three groups (all $P > 0.05$), but the OD of miR-586 inhibition was higher. On the third day, the proliferation activity of miR-586 transfection was visibly higher as against hDPSCs and the Vector ($P < 0.01$). The proliferation activity of miR-586 transfection was visibly

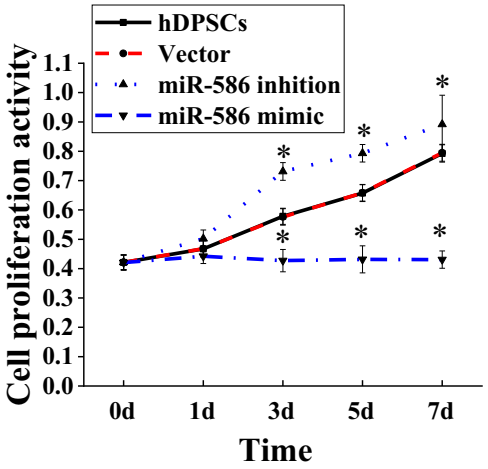

Fig. 5 Suppressing miR-586 expression on the proliferation activity of hDPSCs. Note: As against hDPSCs, $*P < 0.05$

higher as against hDPSCs and the Vector on the 5th to 7th day ($P < 0.05$). However, the proliferation activity of cells in the miR-586 mimic group remained largely unchanged (Fig. 5).

Mineralized Nodule Staining Detection of hDPSCs Cell Differentiation

Observation of microscopic examination results (Fig. 6) revealed that after 14 days of mineralization induction, compared to the hDPSCs group, the staining intensity notably increased in the miR-586 inhibition group, hDPSCs/EPCs group, Vector hDPSCs/EPCs group, and miR-586 inhibition/EPCs group. Conversely, the staining intensity of mineralized nodules remained largely unchanged in both the miR-586 mimic group and miR-586 mimic/EPCs group. Cells in the hDPSCs group (Fig. 6A) exhibited fewer mineralized nodules under inverted microscopy. In contrast, the miR-586 inhibition group (Fig. 6B) showed an increased number of mineralized nodules with deeper reddish-brown staining. The hDPSCs/EPCs group (Fig. 6C) displayed a significantly higher quantity of mineralized nodules compared to the hDPSCs group. Similarly, the Vector hDPSCs/EPCs group (Fig. 6D) exhibited a substantial increase in the number of mineralized nodules with deeper reddish-brown staining compared to the hDPSCs group. The miR-586 inhibition/EPCs group (Fig. 6E) displayed larger and more densely populated mineralized nodules with the deepest reddish-brown staining. In contrast, the miR-586 mimic group (Fig. 6F) exhibited smaller and fewer mineralized nodules. Furthermore, the miR-586 mimic/EPCs group (Fig. 6G) demonstrated a significant reduction in the quantity of mineralized nodules.

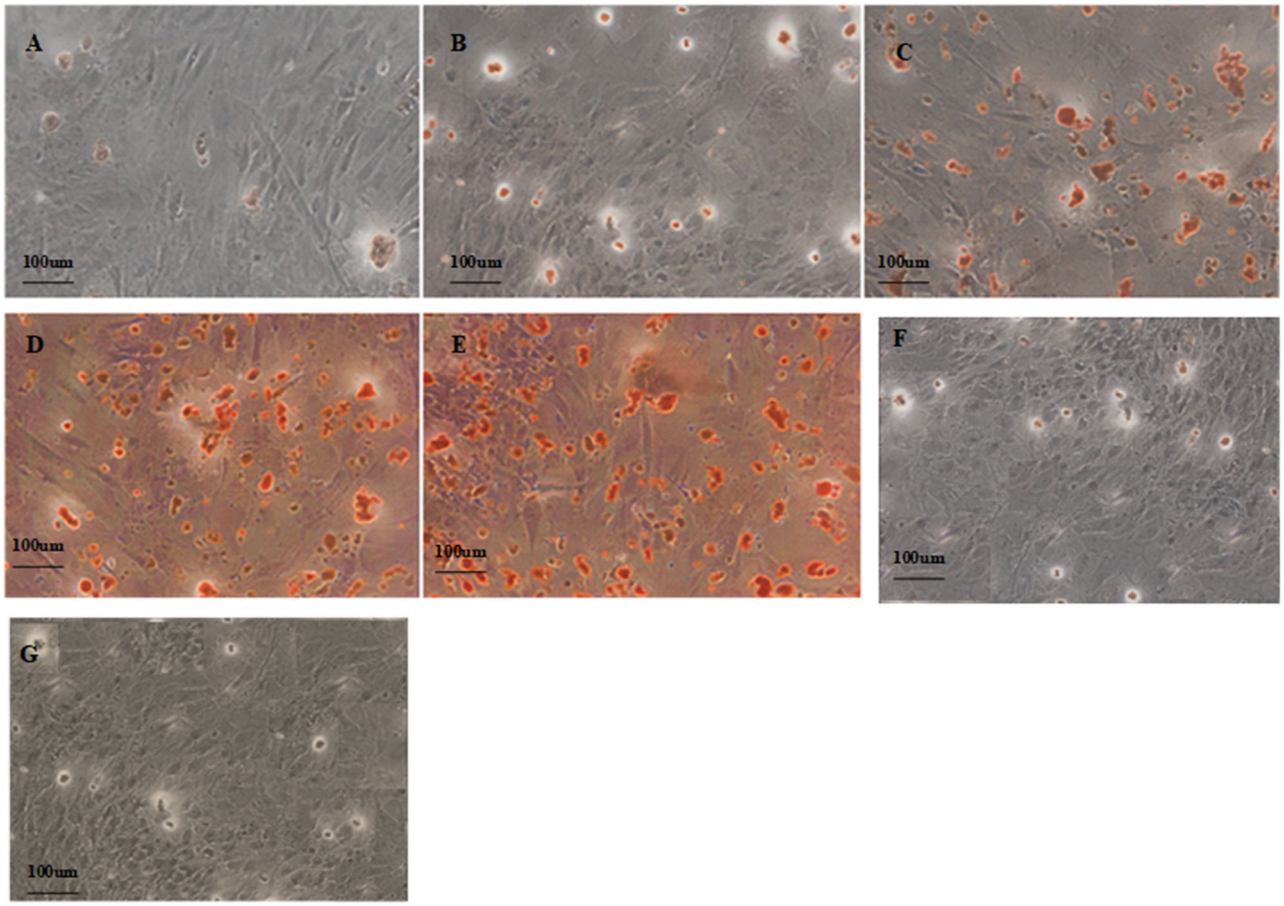

Fig. 6 Mineralized nodule staining for hDPSCs cell differentiation at ×40 magnification. (**A–G** represent hDPSCs group, miR-586 inhibition group, hDPSCs/EPCs group, Vector hDPSCs/EPCs group, miR-586 inhibition/EPCs group, miR-586 mimic group, and miR-586 mimic/EPCs group, respectively.)

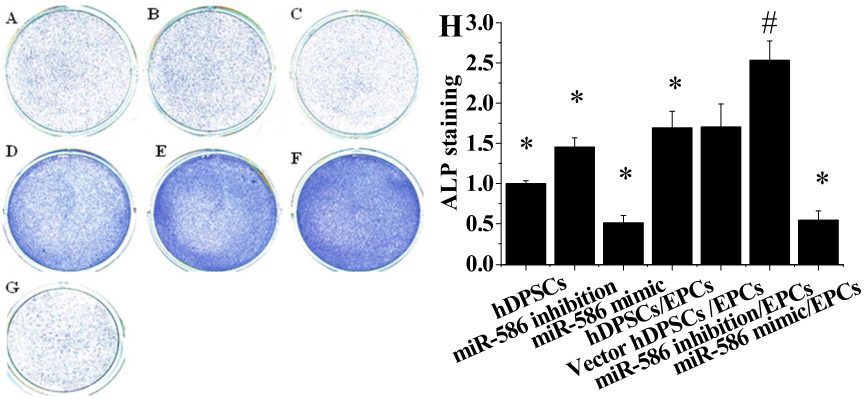

Fig. 7 Comparison of ALP activity among different groups. (**A–G** represent hDPSCs group, miR-586 inhibition group, miR-586 mimic group, hDPSCs/EPCs group, Vector hDPSCs/EPCs group, miR-586 inhibition/EPCs group, and miR-586 mimic/EPCs group, respectively; H represents ALP activity). Note: compared to the hDPSCs group, $*P < 0.05$; compared to the hDPSCs/EPCs group, $\#P < 0.05$

Comparison of ALP Activity Among Different Groups

Observation of the results (Fig. 7) revealed that after 14 days of mineralization induction, compared to the hDPSCs group, the staining intensity notably increased in the miR-586 inhibition group, hDPSCs/EPCs group, Vector hDPSCs/EPCs group, and miR-586 inhibition/EPCs group. Conversely, the staining intensity of the miR-586 mimic group and miR-586 mimic/EPCs group was lower than that of the hDPSCs group and hDPSCs/EPCs group.

RE of DSPP, DMP-1, and ALP mRNA at Different Time Points After Mineralization Induction

The 0 day of mineralization induction was adopted as the Ctrl, and on the third day of mineralizationinduction, the RE

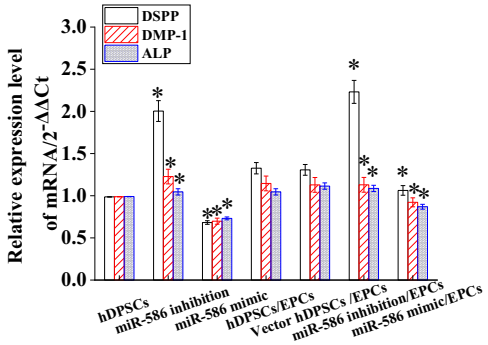

Fig. 8 Contrast of the RE of DSPP, DMP-1, and ALP mRNA on day 0 of mineralization induction. Note: * As against hDPSCs, all $P < 0.05$

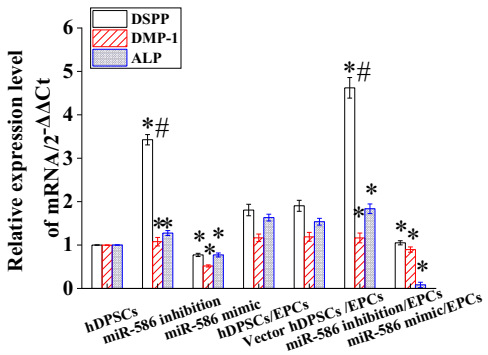

Fig. 9 Contrast of the RE on third day of mineralization induction. Note: * As against hDPSCs, # as against day 0, all $P < 0.05$

of DSPP, DMP-1, and ALP mRNA in hDPSCs was subjected to detection. It suggested that there was no obvious change in the RE in hDPSCs on the third day as against each group on day 0 ($P > 0.05$). The RE in miR-586 inhibition, hDPSCs/EPCs, Vector hDPSCs/EPCs, and miR-586 inhibition/EPCs all suggested an upward trend. In contrast, the miR-586 mimic group exhibited significantly decreased mRNA expression levels of DSPP, DMP-1, and ALP. The expression of miR-586 inhibition and miR-586 inhibition/EPCs was the highest. The RE in miR-586 inhibition/EPCs were visibly higher as against miR-586 inhibition ($P < 0.05$). Moreover, the relative expression levels of DSPP, DMP-1, and ALP mRNA in the miR-586 mimic/EPCs group were significantly reduced compared to the miR-586 mimic group ($P < 0.05$) (Figs. 8 and 9).

On the 7th day of mineralization induction, the RE in hDPSCs were not visibly different from those on day 0 ($P > 0.05$). The RE in miR-586 inhibition, hDPSCs/EPCs, Vector hDPSCs/EPCs, and miR-586 inhibition/EPCs was visibly higher relative to day 0. The relative expression levels of DSPP, DMP-1, and ALP mRNA in the miR-586 mimic group were significantly decreased compared to day 0 ($P < 0.05$). The expression of miR-586 inhibition and miR-586 inhibition/EPCs was the highest. The RE in miR-586 inhibition/EPCs were markedly higher as against miR-586 inhibition (all $P < 0.05$). The relative expression levels of DSPP, DMP-1, and ALP mRNA in the miR-586 mimic/EPCs group were significantly increased compared to the miR-586 mimic group ($P < 0.05$) (Fig. 10).

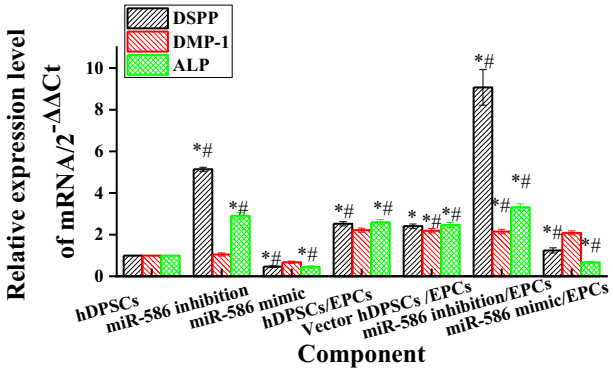

Fig. 10 Contrast of the RE on the 7th day of mineralization induction. Note: * As against hDPSCs, # as against day 0, all $P < 0.05$

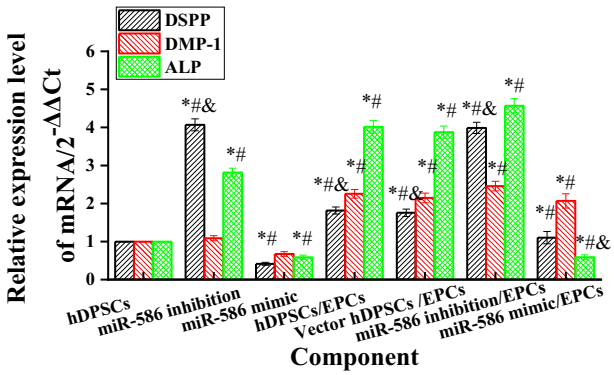

Fig. 11 Contrast of the RE on day 14 of mineralization induction. Note: * as against hDPSCs, # as against day 0, & as against day 7, all $P < 0.05$

On the 14th day of mineralization induction, the RE of DSPP, DMP-1, and ALP mRNA in hDPSCs were not markedly different from those on day 0 ($P > 0.05$). The RE of DSPP mRNA in miR-586 inhibition, hDPSCs/EPCs, Vector hDPSCs/EPCs, and miR-586 inhibition/EPCs was markedly lower relative to day 7; the RE of DSP, PDMP-1, and ALP mRNA was markedly higher relative to day 0 (all $P < 0.05$).The relative expression levels of DSPP, DMP-1, and ALP mRNA in the miR-586 mimic group showed no significant change compared to day 7. However, in the miR-586 mimic/EPCs group, the relative expression levels of DSPP, DMP-1, and ALP mRNA were significantly decreased compared to day 7 ($P < 0.05$) (Fig. 11).

WB for Detection of the Level of DSPP Protein

The protein level of DSPP in the five groups suggested an upward tendency on day 0 to day 7, and the protein level of DSPP in the five groups on day 4 and day 7 of

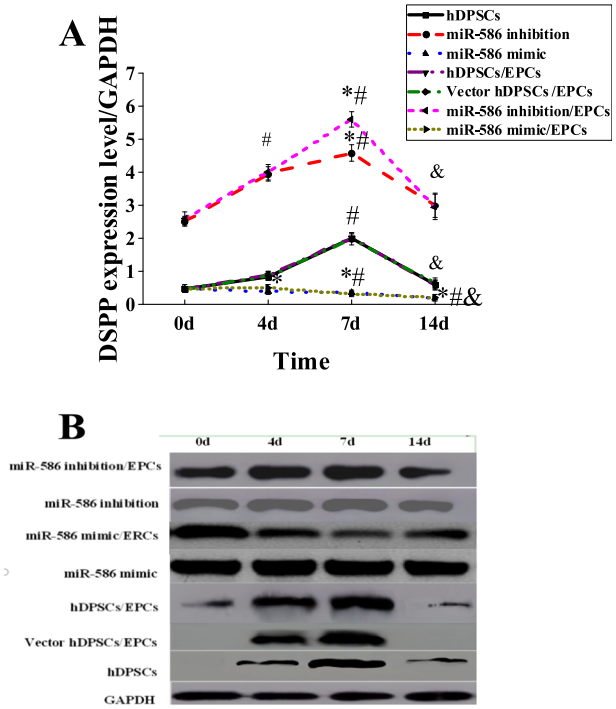

Fig. 12 Contrast of DSPP protein expression. (**A** represents the expression level of DSPP, while **B** represents the WB image of DSPP expression.). Note: * as against hDPSCs, # as against day 0, & as against day 7, all $P < 0.05$

mineralization induction were markedly higher relative to day 0. In addition, DSPP protein expression in miR-586 inhibition/EPCs and miR-586 inhibition were markedly higher as against the other three groups. On the 14th day, the protein expression of DSPP in the five groups were markedly lower relative to the 7th day (all $P < 0.05$). However, DSPP protein was all higher relative to day 0 ($P < 0.05$), and the miR-586 mimic/EPCs group exhibited a noticeable downward trend in DSPP protein expression levels compared to the miR-586 mimic group ($P < 0.05$) (Fig. 12).

Discussion

Pulp regeneration is of great significance for patients with dental pulp diseases, which can protect the teeth. In the case of tooth infection or damage, tooth extraction may be required. Pulp regeneration technology is expected to help patients avoid tooth loss [17]. Tissue regeneration induction technology plays a major role in dental pulp regrowing. This article adopted co-culture system and suppressing miR-586 expression to discuss the function and action of miR-586 in DPSCs differentiation into dentin-like cells. There are various stem cells in the body, which have high differentiation potential and self-renewal ability, and can differentiate into specific types of cells through gene regulation [18]. MicroRNAs regulate gene expression by binding to the 3' untranslated region (3'UTR) of target mRNAs, leading to mRNA degradation or translation inhibition. miR-586 may directly bind to the mRNA of key osteogenic or odontogenic differentiation genes, participating in signaling pathway regulation, influencing the expression of cell cycle-related genes, regulating cell proliferation status, and thereby impacting the differentiation process.

In this article, miR-586 lentiviral expression vector was established, and the venom for transfection was prepared by 293 T cells, and then the venom was transfected into hDPSCs. It suggested that under the impact of miR-586 lentiviral expression inhibition vector, the RE of miR-586 gene in empty and normal cells was not markedly different, $0.96/2^{-\Delta\Delta Ct}$ and $0.99/2^{-\Delta\Delta Ct}$, respectively. The RE of miR-586 gene in hDPSCs transfected with miR-586 inhibition lentiviral vector was markedly lower as against normal cells, indicating that the successful construction of lentiviral vector and the miR-586 inhibition lentiviral vector successfully reduced the expression level of miR-586. The empty lentiviral vector had no visible outcome on the expression of miR-586. Then, the impact of miR-586 lentivirus expression inhibition vector on the expression of DSPP protein in hDPSCs was explored. It suggested that the expression of DSPP protein in hDPSCs transfected with miR-586 lentivirus expression inhibition vector was markedly raised, indicating that the suppressing miR-586 expression could increase the expression of DSPP. DSPP is a protein that promotes biomineralization and is related to the repair of DPT [18].

Figueredo et al. investigated the role of DSPP in dental and craniofacial development using DSPP knockout and C57BL/6J wild-type mice, with DSPP being identified as a protein essential for normal mineralization of dental and craniofacial tissues [19]. DSPP has the effect of promoting the mineralization of calcium and phosphorus in dentin, which makes the dentin hard and has enough hardness to resist chewing and occlusal pressure. Lack of DSPP leads to insufficient mineralization of dentin, making it soft and susceptible to acid and bacterial erosion, thereby increasing the risk of dental caries [20–22]. The softening and fragility of dentin increases the risk of exposing the neural tissue underlying the dentin to irritants, which may lead to dentin sensitivity, and patients may experience pain or discomfort [23]. In this article, it was found that on the 14th day of mineralization induction, the relative expression of DSPP mRNA in cells of the miR-586 inhibition group, hDPSCs/EPCs group, Vector hDPSCs/EPCs group, and miR-586 inhibition/EPCs group was significantly decreased compared to the 7th day but was still significantly higher than on the 0th day ($P < 0.05$). This is similar to the

aforementioned studies, suggesting that the inhibition of miR-586 expression could promote the expression level of cellular DSPP, thereby having a positive impact on the biomineralization process and the repair of pulp tissue. Additionally, this article also found that the proliferative activity of the three groups of cells showed an upward trend 1–7 days after transfection with the lentiviral plasmid. Specifically, on the 3rd day, the proliferative activity of cells in the miR-586 inhibition group was significantly higher than that in the hDPSCs group and the Vector group ($P < 0.01$), and from the 5th to the 7th day, the proliferative activity of cells in the miR-586 inhibition group was significantly higher than that in the hDPSCs group and the Vector group ($P < 0.05$). This indicates that the molecular mechanism by which the inhibition of miR-586 enhances the proliferative activity of hDPSCs cells by promoting the secretion of cellular DSPP, especially in the short term, may have a positive effect on cell proliferation. It is thus speculated that non-coding RNA may have an antagonistic outcome on the odontoblast differentiation of hDPSC, and the results in this article are consistent with expectations. In the mineralization induction of hDPSCs, the number and color of mineralized nodules were markedly deepened in the miR-586 inhibition group, indicating that suppressing miR-586 gene expression may promote the formation of mineralized nodules. Suppressing miR-586 expression may promote the expression of DSPP, which is able to repair dentin and thus promote the formation of mineralized nodules. In this article, hDPSC/EPCs co-culture method was adopted to conduct an exploration of the impact of miR-586 on the related genes of hDPSCs during the differentiation of hDPSCs into dentin cells. Suppressing miR-586 expression could promote the expression of DSPP protein in hDPSCs, which was consistent with the above results.

DMP-1 and ALP also act in the differentiating hDPSCs, and these sequences can promote the binding of proteins to hydroxyapatite, thereby regulating biomeramalization [24]. DMP-1 is a dentin-specific protein, which can promote the mineralization of dentin [25]. During the differentiation of hDPSCs into dentin cells, DMP-1 can increase the deposition of calcium and phosphorus, thereby promoting the hardening and mineralization of dentin. ALP has the outcome of promoting phosphate metabolism, and when hDPSCs differentiate into dentin cells, the activity of ALP increases and helps to catalyze the degradation of phosphate, thus providing phosphorus and calcium ions required for the mineralization process [26–28]. In addition, ALP also act in maintaining appropriate pH conditions, which is essential for the deposition of calcium phosphate salts and dentin mineralization. In this article, it was found that on the 7th day of mineralization induction, the relative expression levels of DSPP, DMP-1, and ALP mRNA in cells of the miR-586 inhibition group, hDPSCs/EPCs group, Vector hDPSCs/EPCs group, and miR-586 inhibition/EPCs group had significantly increased compared to day 0 ($P < 0.05$). This suggests that the inhibition of miR-586 expression could promote the expression levels of DMP-1 and ALP mRNA, thereby advancing the biomineralization process of hDPSCs cells and enhancing their differentiation potential. MiR-586 acts as a negative regulator by suppressing the expression of key genes such as DMP-1, ALP, and DSPP, thereby influencing the processes of osteogenic and odontogenic differentiation. Inhibiting the expression of miR-586 can alleviate this inhibitory effect, promoting the expression of genes related to osteogenic and odontogenic differentiation and accelerating the mineralization process.

MiR-586 has been shown to regulate cell biological processes in many cell types, and this article confirmed that it also plays a key role in the differentiation of DPSCs. This article found miR-586 could target DSPP to regulate some key genes and proteins. However, the limitations of the study lie in its exclusive focus on in vitro cell models, without involving animal models or clinical studies. Therefore, further validation is needed to assess the actual efficacy and safety in vivo. Future research should consider expanding to in vivo models to comprehensively evaluate the potential application of miR-586 in dental pulp regeneration.

Conclusion

In summary, the results suggested that suppressing miR-586 had an obvious outcome on hDPSCs. Suppressing miR-586 expression could upregulate the expression of DSPP, promote the proliferative activity of hDPSCs, promote the formation of dentin mineralized nodules, and enhance the expression of DMP-1 and ALP mRNA. The exploration of the function of miR-586 in tooth regeneration and restoration is meaningful. In the future, this mechanism can be further explored to provide more research directions and application potential for regenerative medicine in the oral field.

Data Availability

The datasets used and/or analyzed in the present study are available from the corresponding author upon reasonable request.

Author contributions GP, QZ, CP and YZ participated the design, supervision and editing, and resources, writing of original draft, experimental implementation, and data statistics and analysis. All authors read and approved final manuscript.

Compliance with Ethical Standards

Conflict of Interest The authors declare no competing interests.

References

1. Samir, P. V., Mahapatra, N., Dutta, B., Bagchi, A., Dhull, K. S., & Verma, R. K. (2023). A correlation between clinical classification of dental pulp and periapical diseases with its pathophysiology and pain pathway. *International Journal of Clinical Pediatric Dentistry*, *16*, 639–644.
2. Yan, H., De Deus, G., Kristoffersen, I. M., Wiig, E., Reseland, J. E., Johnsen, G. F., Silva, E. J. N. L., & Haugen, H. J. (2023). Regenerative endodontics by cell homing: A review of recent clinical trials. *Journal of Endodontics*, *49*, 4–17.
3. Widbiller, M., Knüttel, H., Meschi, N., & Durán-SindreuTerol, F. (2023). Effectiveness of endodontic tissue engineering in treatment of apical periodontitis: A systematic review. *International Endodontic Journal*, *56*, 533–548.
4. Luzuriaga, J., García-Gallastegui, P., & García-Urkia, N., et al. (2022). Osteogenic differentiation of human dental pulp stem cells in decellularised adipose tissue solid foams. *European Cells & Materials*, *43*, 112–129.
5. Merkel, A., Chen, Y., Villani, C., & George, A. (2023). GRP78 promotes the osteogenic and angiogenic response in periodontal ligament stem cells. *European Cells & Materials*, *45*, 14–30.
6. Maity, J., Barthels, D., & Sarkar, J., et al. (2022). Ferutinin induces osteoblast differentiation of DPSCs via induction of KLF2 and autophagy/mitophagy. *Cell Death & Disease*, *13*, 452.
7. Bar, J. K., Lis-Nawara, A., & Grelewski, P. G. (2021). Dental pulp stem cell-derived secretome and its regenerative potential. *International Journal of Molecular Sciences*, *22*, 12018.
8. ÖzgülÖzdemir, R. B., Özdemir, A. T., & Kırmaz, C., et al. (2021). Age-related changes in the immunomodulatory effects of human dental pulp derived mesenchymal stem cells on the CD4+ T cell subsets. *Cytokine*, *138*, 155367.
9. Li, X., Hou, J., Wu, B., Chen, T., & Luo, A. (2014). Effects of platelet-rich plasma and cell coculture on angiogenesis in human dental pulp stem cells and endothelial progenitor cells. *Journal of Endodontics*, *40*, 1810–1814.
10. Zheng, H., Zhang, X., & Fu, J., et al. (2023). CHIP inhibits odontoblast differentiation through promoting DLX3 polyubiquitylation and degradation. *Develop*, *150*, 200848.
11. Liu, M. M., Li, W. T., & Xia, X. M., et al. (2021). Dentine sialophosphoprotein signal in dentineogenesis and dentine regeneration. *European Cells & Materials*, *42*, 43–62.
12. Zhang, W., & Yuan, X. (2022). MicroRNA-20a elevates osteogenic/odontoblastic differentiation potential of dental pulp stem cells by nuclear factor-κB/p65 signaling pathway via targeting interleukin-8. *Archives of Oral Biology*, *138*, 105414.
13. Wang, J., Zheng, Y., & Bai, B., et al. (2020). MicroRNA-125a-3p participates in odontoblastic differentiation of dental pulp stem cells by targeting Fyn. *Cytotechnology*, *72*, 69–79.
14. Zhang, D., Liu, X., & Li, Y., et al. (2021). LINC01189-miR-586-ZEB1 feedback loop regulates breast cancer progression through Wnt/β-catenin signaling pathway. *Molecular Therapy - Nucleic Acids*, *25*, 455–467.
15. Liu, C., Yang, J., Zhu, F., Zhao, Z., & Gao, L. (2022). Exosomal circ_0001190 regulates the progression of gastric cancer Via miR-586/SOSTDC1 Axis. *Biochemical Genetics*, *60*, 1895–1913.
16. Yu, A., Zhang, J., & Mei, Y., et al. (2020). Correlation between single nucleotide polymorphisms of an miRNA binding site in the 3'UTR of PTEN and risk of cervical cancer among the Han Chinese. *Genetic Testing and Molecular Biomarkers*, *24*, 381–389.
17. Hammouda, D. A., Mansour, A. M., Saeed, M. A., Zaher, A. R., & Grawish, M. E. (2023). Stem cell-derived exosomes for dentin-pulp complex regeneration: a mini-review. *Restorative Dentistry and Endodontics*, *48*, e20.
18. Ruan, Q., Tan, S., Guo, L., Ma, D., & Wen, J. (2023). Pre-vascularization techniques for dental pulp regeneration: potential cell sources, intercellular communication and construction strategies. *Frontiers in Bioengineering and Biotechnology*, *11*, 1186030.
19. Figueredo, C. A., Abdelhay, N., Ganatra, S., & Gibson, M. P. (2022). The role of dentin sialophosphoprotein (DSPP) in craniofacial development. *Journal of Oral Biology and Craniofacial Research*, *12*, 673–678.
20. Ye, J., Wang, Y., & Zhu, Q., et al. (2021). Primary observation of the role of posttranslational modification of dentin sialophosphoprotein (DSPP) on postnatal development of mandibular condyle in mice. *Archives of Oral Biology*, *125*, 105086.
21. Ihn, H. J., Kim, J. A., & Lim, J., et al. (2021). Bobby sox homolog regulates tooth root formation through modulation of dentin sialophosphoprotein. *Journal of Cellular Physiology*, *236*, 480–488.
22. Jalal Hussein, F., SherdlSaleem, S., & AbdulazizMerdad, K. (2023). Relationship between dental caries experience and the levels of streptococcus mutans and lactobacillus in saliva of pregnant women. *Cellular and Molecular Biology*, *69*, 148–155.
23. Li, B., Xu, J., & Ai, R., et al. (2023). Safe and durable treatment of dentin hypersensitivity via nourishing and remineralizingdentin based on β-chitooligosaccharidegraft derivative. *Small*, *19*, e2300359.
24. Whyte, M. P., Amalnath, S. D., & McAlister, W. H., et al. (2020). Hypophosphatemicosteosclerosis, hyperostosis, and enthesopathy associated with novel homozygous mutations of DMP1 encoding dentin matrix protein 1 and SPP1 encoding osteopontin: The first digenic SIBLING protein osteopathy. *Bone*, *132*, 115190.
25. Beniash, E., Deshpande, A. S., Fang, P. A., Lieb, N. S., Zhang, X., & Sfeir, C. S. (2011). Possible role of DMP1 in dentin mineralization. *Journal of Structural Biology*, *174*(1), 100–106.
26. Sismanoglu, S., & Ercal, P. (2023). Effects of calcium silicate-based cements on odonto/osteogenic differentiation potential in mesenchymal stem cells. *Australian Endodontic Journal*, *49*, 66–74.
27. Qiu, M., Bae, K. B., & Liu, G., et al. (2023). Osteolectinpromotes odontoblastic differentiation in human dental pulp cells. *Journal of Endodonticsont*, *49*, 1660–1667.
28. Miyano, Y., Mikami, M., Katsuragi, H., & Shinkai, K. (2023). Effects of Sr2+, BO33-, and SiO32- on differentiation of human dental pulp stem cells into odontoblast-like cells. *Biological Trace Element Research*, *201*, 5585–5600.